

RECOVERY OF ZINC FROM ZINC OXIDE DUST CONTAINING MULTIPLE METAL ELEMENTS BY CARBOTHERMAL REDUCTION

F.-G. Lei ^{a,b,c}, M.-T. Li ^{a,*}, C. Wei ^a, Z.-G. Deng ^a, X.-B. Li ^a, G. Fan ^a

^a Faculty of Metallurgical and Energy Engineering, Kunming University of Science and Technology, Kunming, China

^b State Key Laboratory of Comprehensive Utilization of Low-Grade Refractory Gold Ores, Xiamen, China

^c Zijin Mining Group Xiamen Zijin Mining and Metallurgy Technology Co.,Ltd., Xiamen, China

(Received 02 November 2020; accepted 19 October 2021)

Abstract

A carbothermal reduction process simulating EAF process is used to handle the zinc oxide dust, and the zinc in the dust can be extracted and recovered efficiently. The crude zinc and lead-tin alloy were obtained finally. The effects of temperature, holding time, and reductant dosage on zinc volatilization rate were investigated, and the "Pelletizing - Calcination-Carbothermic reduction" experiment was conducted. The results found the optimal reduction condition was as follows: the temperature of 1300°C, reductant dosage of 14.04%, and holding time of 120 min. After the calcination at 900°C for 120 min, the removal rates of fluorine, chlorine, and sulfur in the dust were 98.18%, 96.38% and 28.58% respectively, and the volatilization rate of zinc was 99.83% in the reduction process. The zinc content of the crude zinc was 68.48%.

Keywords: Zinc oxide dust; Carbothermal reduction; Volatilization; Condensation; Recovery

1. Introduction

Zinc oxide dust (ZOD)—produced from rotary hearth furnaces, Waelz kilns, W-Zn-O furnaces, and fuming furnaces—contains multiple metal elements and is a valuable secondary zinc oxide resource [1-4]. The zinc content in ZOD is high and the main phase of zinc is zinc oxide. ZOD usually contains lead, cadmium, tin, other non-ferrous metals, and a small amount of rare indium, silver metals [5-9]. Additionally, ZOD has different levels of undesirable elements, fluorine and chlorine [4]. Wasting the vast quantities of valuable secondary resources in ZOD takes up space that could instead be used for farmland, and severely pollutes the surrounding environment [10]. ZOD offers considerable recycling value and is profitable for smelting plants.

Currently, researchers employ hydrometallurgical methods including acid, alkaline, and ammonia leaching to treat ZOD [11, 12]. Sulfuric acid leaching is the mainstream method for industrial recycling of ZOD worldwide. In acid leaching, zinc in ZOD is leached with sulfuric acid (H₂SO₄) and recovered from the pregnant leach solution via electrowinning, and lead enters the leach residue as sulphate [13-16].

Sulfuric acid leaching is suitable for ZOD

containing relatively low concentrations of lead. However, at high lead concentrations, substantial quantities of the lead convert to lead sulfate, which could form a loose structure. As a result, the zinc oxide or zinc ferrite may be encapsulated [16-18]. This may result in a poor zinc leaching rate [16]. Increasing the liquid/solid ratio can counteract the encapsulation effect to some extent through magnifying the mass transfer and diffusion [19-21]. However, excessively increasing the liquid/solid ratio changes the pH, resulting in the generation of a silica gel. This is disadvantageous to solid-liquid separation. Furthermore, the Zn²⁺ concentration in the leach solution, generally 170–200 g/L during electrowinning, decreases to an extent that hinders electrowinning [22]. Additionally, the substantial amount of leach residue is produced in the leaching stage because of the high content lead in ZOD [13, 23, 24]. The leach residue includes high concentration of heavy metals such as lead, zinc, nickel, cadmium, manganese, and arsenic [24-27]. Since the leach residue is classified as a hazardous waste [13, 28], it's needed to be disposed through such as, the Outotec Ausmelt technology, and the Waelz Kiln process [29]. For the whole process, sulfuric acid leaching and the disposal of the leach residue, the circulation of sulfur,

* Corresponding author: liminting@163.com



i.e., sulfuric acid→leach residue→sulfuric acid, which increases the cost. Consequently, lead and zinc are recovered asynchronously in sulfuric acid leaching, which increases the cost. Besides, in hydrometallurgical method, the large consumption of leaching agent and disposal of a large amount of wastewater also increase cost [26], and the simultaneous separation and recovery of valuable elements and the recovery of tin are difficult to achieve.

The generation of arsine is also a health and safety issue that cannot be ignored. Fluorine and chlorine in ZOD would bring significant detriments to electrowinning, such as aluminum cathode and anode grid corrosion [4, 30]. Thus, Fluorine and chlorine have to be removed in an additional step. In general, the concentrations of fluorine and chlorine ion in electrolytes must meet electrolysis requirements ($F < 80\text{mg/L}$, $Cl < 100\text{mg/L}$) in the electrowinning [4].

The ZOD produced from blast furnace slag treated by a rotary hearth furnace is from a secondary resource processing plant in Yunnan province, and the yield of the ZOD is about 600 t annually. The lead, fluorine and chlorine content in the ZOD are high. Therefore, the ZOD is not readily amenable to traditional hydrometallurgical method, and synchronous recycling of zinc, lead, and tin in the ZOD is hard to achieve with it. Pyrometallurgical processes such as blast furnace and electric arc furnace (EAF) methods can be used to dispose ZOD. However, the blast furnace is suitable for treating large-scale material, which has no advantage for disposing the ZOD in economy. In addition, if the ZOD is used as a charge mixture in blast furnace process, tin in the ZOD is difficult to be recovered due to dilution of tin. The treatment scale of EAF is flexible, and it can achieve synchronous recycling of zinc, lead and tin in the ZOD. At present, the EAF method is often used to treat zinc calcine with a lead content of not more than 5%. The research object in this paper is a zinc oxide dust with a lead content of 27.65%. This work is a laboratory-scale attempt to treat zinc oxide dust with high lead content by EAF method.

A carbothermal reduction process simulating EAF process is used to handle the ZOD in this work. In the process, zinc oxide can turn into zinc vapor which will transform into crude zinc in the condenser. Most lead and tin element are at the bottom of furnace as lead-tin alloy, and part of lead and tin go inside of the crude zinc through entrainment of zinc vapor. Thus, lead and tin are separated from zinc, and recovered in the form of lead-tin alloy. Zinc is recovered in the form of

crude zinc. Lead-tin alloy and crude zinc can go through the refining system and produce refined lead and refined zinc in industry, respectively. The main objective of this work is to investigate volatilization behavior of zinc in carbothermal reduction process. The effects of temperature, holding time, and reductant dosage on zinc volatilization rate were investigated, and the “Pelletizing – Calcination – Carbothermal reduction” experiment was conducted.

2. Experimental

2.1. Raw materials and its characterization

The ZOD was obtained from a secondary resource processing plant in Yunnan province, China. The zinc content in the ZOD is 40.44%. Table 1 shows the main chemical constituents of the dust. The X-ray diffraction analysis of the ZOD is given in the Figure 1. As shown in Fig 1, zinc in the ZOD is mainly in the

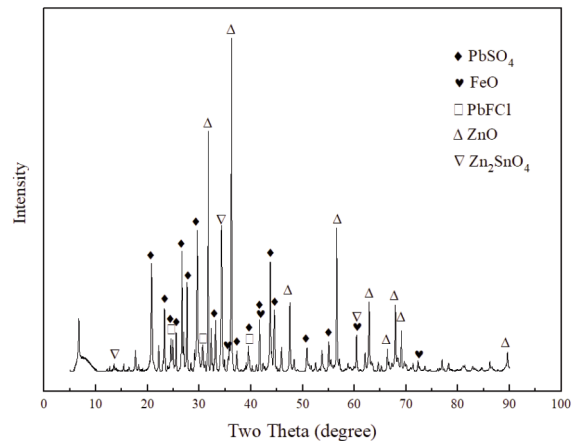


Figure 1. X-ray diffraction analysis of the ZOD

form of zinc oxide, and some zinc combines with tin and oxygen to form zinc stannate (Zn_2SnO_4). The main form of lead is lead sulfate, and a little lead exists in the form of PbFCl . The main chemical analysis of the reductant used as reductant in the work is given in the Table 2. The carbon content in the reductant exceeds 98.5% (Table 2).

Table 2. Main chemical constituents of reductant

| Composition | C | N | S | M | A | V |
|-------------|-------------|------------|------------|------------|------------|------------|
| Wt. % | ≥ 98.5 | ≤ 0.1 | ≤ 0.5 | ≤ 0.5 | ≤ 0.8 | ≤ 0.8 |

The dissolution experiments were performed to quantitate soluble sulfur—zinc sulfate—in the dust. 50 g of the dust was dissolved in the distilled water at a liquid/solid ratio of 5 mL/g. The slurry was stirred

Table 1. Chemical analysis of the zinc oxide dust

| Composition | Zn | Pb | Sn | As | S | F | Cl | Ag | In |
|-------------|-------|-------|------|-----|------|------|------|-------|--------|
| Wt. % | 40.44 | 27.65 | 3.70 | 0.5 | 3.26 | 0.80 | 0.88 | 69g/t | 265g/t |



for 180 min at 300 r/min and 25°C with a magnetic stirrer, the slurry was filtered, and then collected and analyzed. The results found that the average removal percent of sulfur was 2.15%, which demonstrated that sulfur was principally in the form of lead sulfate, and there was almost no soluble sulfur—zinc sulfate—because of the low removal rate of sulfur. This corresponds to the XRD pattern of the ZOD.

2.2. Calcination

The ZOD was sent to the lab-scale disk pelletizer for pelletizing. The pellets were loaded into a corundum crucible and were dried in a muffle furnace at 150°C for 120 min. After drying, the 2000 g pellets with a size of 3~8 mm were loaded into a corundum crucible, and the corundum crucible with the pellets was sent into the muffle furnace and was calcined at 900°C for 60 min. After calcination, the pellets were preserved as raw material.

2.3. Carbothermal reduction experiment

The main equipment in our work was an electric heated horizontal tube furnace, and the schematic diagram of the experimental process is shown in Fig 2. The raw material of the single factor condition experiment was the dust, and the raw material dosage was 50 g. The raw material of the “Pelletizing - Calcination-Carbothermal reduction” experiment was the pellets calcined, and the raw material dosage was 1000 g.

The raw material and carbonaceous reducer were blended in the required proportions. In this work, the reductant dosage is defined as the mass ratio of reductant and raw material. The mixture of the dust and reductant was enclosed in a graphite crucible called reactor, then the reactor was connected to three graphite crucibles called three-level condensers. The entire reaction setup composed of the reactor and three-level condensers was loaded into the high-

temperature zone of the horizontal tube furnace. Subsequently, when temperature rose to the target temperature, the constant temperature was maintained for a set period of time. After heat preservation, the entire reaction setup naturally cooled to room temperature and was taken out of the furnace. Both the residue in the reactor and the condensate in the three-level condensers were collected respectively and analyzed. The residue was separated into lead-tin alloy and slag, and the condensate was separated into crude zinc and condensation powder.

2.4. Analysis methods

The chemical composition of the ZOD was analyzed with an inductively coupled plasma instrument (Optima 8000 Leeman, USA). The disodium EDTA titration method and the EDTA titration method were used to determine the zinc and lead content, respectively, in the solid products.

The phase constituents of solid materials were identified by XRD (Rigaku-TTR III, Japan). The morphology of solid materials was observed with an SEM (HitachiS-3400N, Japan).

3. Results and discussion

3.1. Thermodynamic Analysis

3.1.1. Reduction of zinc oxide

Eqs. 1–3 list the reduction equations that pertain to zinc oxide during carbothermal reduction and the relationship between the standard Gibbs free energy

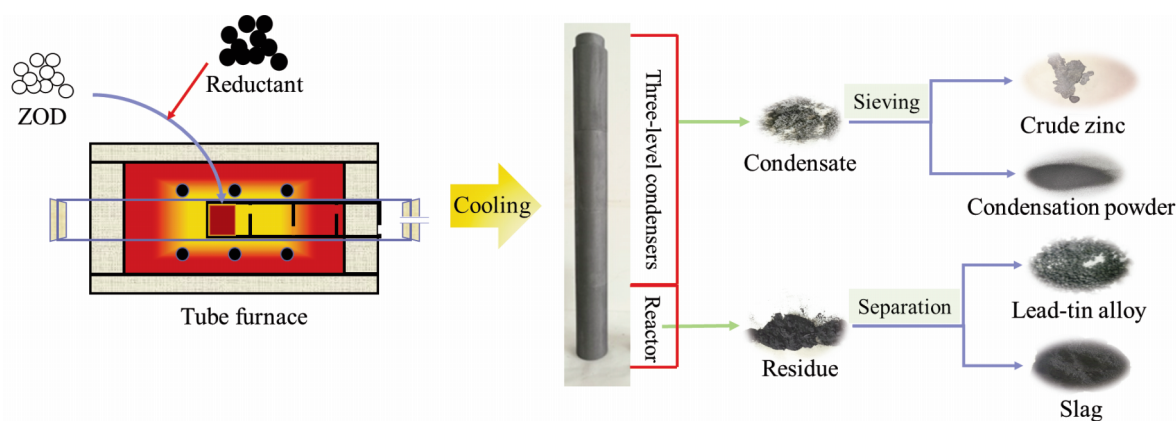
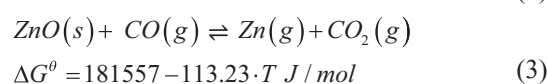
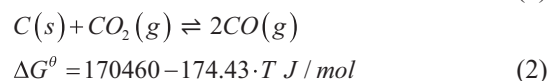
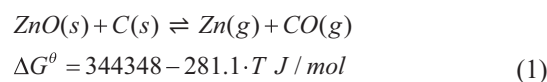


Figure 2. The schematic diagram of the experimental process

change (ΔG°) of Eqs. 1–4 and the temperature (T) [31], so the function relationship between ΔG° of Eqs. 1–3 and T can be drawn, as expressed in Fig 3.

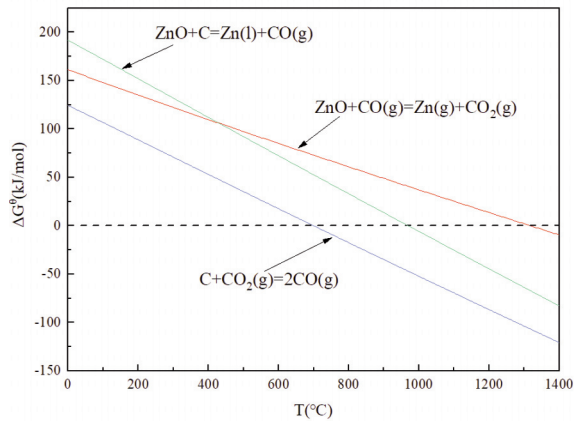


Figure 3. Function relationship between ΔG° of Eqs. 1–4 and T

The theoretical initial reaction temperature of Eq. 1 is lower than that of Eq. 3 (Fig 3). Thus, Eq. 1 occurs before Eq. 3 in theory, and Eq. 3 takes place at 1203°C. However, in industrial EAF method, Eq. 3 predominates when temperature exceeds 1000°C. Maintenance of Eq. 3 is not only related to temperature but also to the partial pressure of carbon monoxide offered by Boundouard reaction (Eq. 2) [32]. As illustrated in Fig 4, when the partial pressure of zinc vapor is set as 0.5 in the furnace, the partial pressure of carbon monoxide offered by Eq. 2 has exceeded the partial pressure of carbon monoxide needed by Eq. 3 at approximately 926°C, which makes Eq. 3 take place smoothly. Actually, the partial pressure of zinc vapor in EAF is usually 0.05~0.06.

For Eq. 3, the apparent activation energy of the gas diffusion step is greater than that of other restrictive steps in zinc reduction [33]; thus, the higher partial pressure of CO in the CO/(CO+CO₂) benefits Eq. 3 [34].

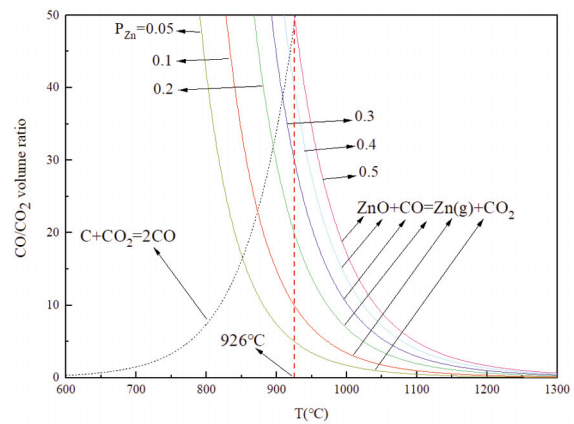


Figure 4. Effect of CO/CO₂ volume ratio on Eq. 3

The equilibrium module of HSC Chemistry 6.0 is used to calculate the multi-component equilibrium composition of the system ZnO–C (2:1) over a range of temperatures at 1 atm [35]. Fig 5(a) shows the solid carbon content clearly decreased at temperatures greater than 800°C. Meanwhile, Fig 5(b) shows the condensed state of zinc started to appear. The quantity of the condensed state zinc reaches a maximum at 907°C. After 907°C, a mass of zinc vapor is generated, because the condensed state zinc volatilizes and Eq. 3 intensifies. The partial pressure of carbon monoxide increases remarkably at 800°C, and reached a high level at approximately 910°C. Solid carbon in direct contact with zinc oxide is nearly used up at 910°C, which weakens the solid–solid reactions, Eq. 1. Concurrently, the partial pressure of carbon monoxide sharply decreases, and the quantity of zinc oxide and zinc vapor decreases and increases respectively at similar rates. This demonstrates that the reaction mechanism changes over time. Hence, Eq. 1 predominates before 910°C, and Eq. 3 becomes the predominant reaction after 910°C. This is consistent with the aforementioned thermodynamic analysis.

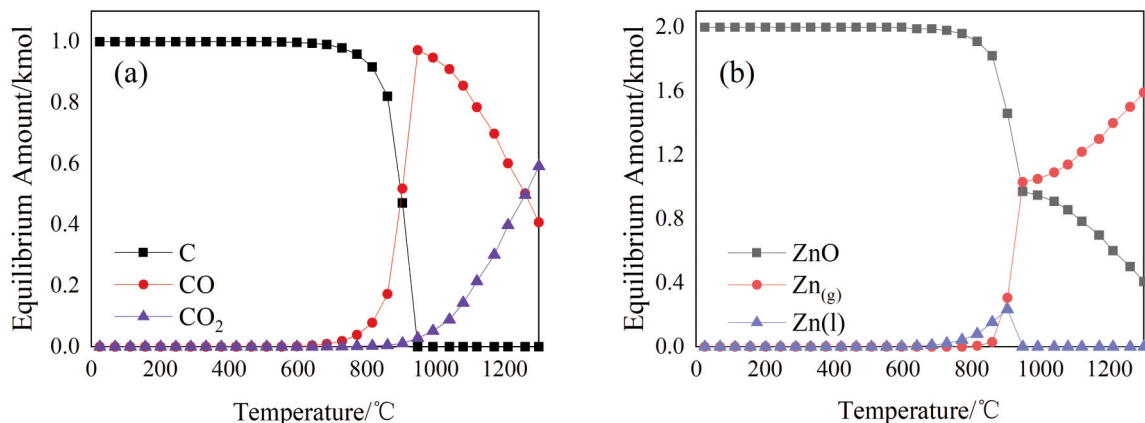


Figure 5. Multi-component equilibrium composition of the system ZnO–C (2:1): (a) Carbon species (b) Zinc species

3.1.2. Effect of sulfur on zinc reduction behavior

At high temperature, sulfur may influence zinc behavior, i.e. the reduction and volatilization of zinc, through Eq. 4 and 5. The relationship between ΔG^θ of Eqs. 4-6 and T was given in Fig 6.

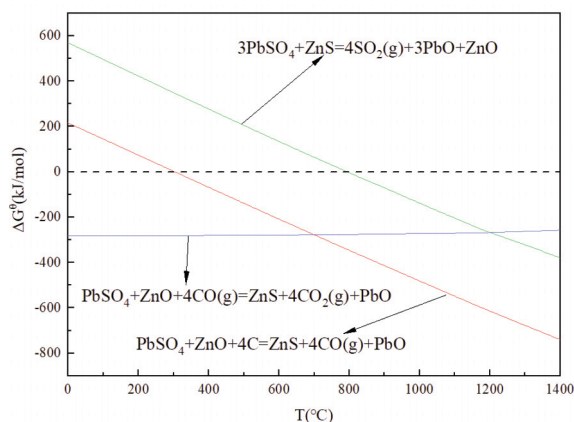
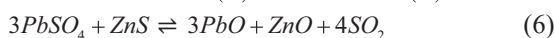
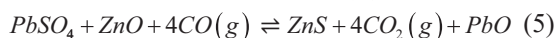


Figure 6. Function relationship between ΔG^θ of Eqs. 4–6 and T

Eqs. 4 and 5 can take place when the temperature exceeds 750°C (Fig 6). Sulfur captures some zinc in the ZOD and forms zinc sulfide, hindering the reduction of zinc. Furthermore, zinc sulfide can react with lead sulfate theoretically at temperatures greater than 850°C (Eq 5), which indicates Eq. 6 can counteract the effect of Eqs. 4 and 5 to some extent. In addition, the volatility of zinc sulfide is weaker than that of metallic zinc, so sulfur could reduce the volatilization rate of zinc. In conclusion, the existence of sulfur in the ZOD can attenuates the reduction and volatilization rate of zinc via the generation of zinc sulfide.

3.2. Carbothermal reduction experiments

3.2.1. Effect of temperature on zinc volatilization

The effect of temperature on volatilization rate of zinc was investigated at a holding time of 120 min and a reductant dosage of 19.14%, and the temperature was set at 800°C, 850°C, 900°C, 950°C, 1000°C, 1050°C, 1100°C, 1150°C, 1250°C, and 1300°C. The result was shown in Fig 7(a).

Fig 7(a) indicated that the zinc content of the residue in the reactor decreased in accordance with increasing temperature. When the temperature was 1300°C, the minimum zinc content of the residue in reactor was 0.061 wt.%. The volatilization rate of zinc

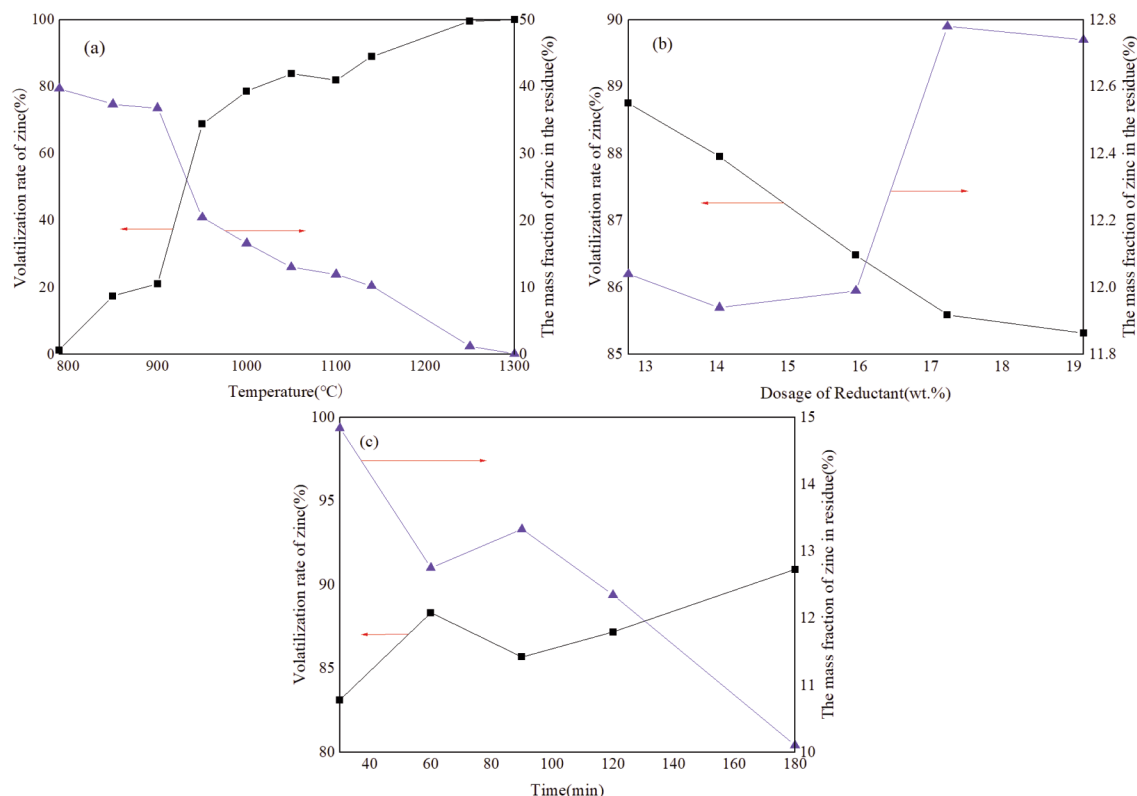


Figure 7. Effects of parameters on volatilization rate of zinc: (a) temperature (b) reductant dosage (c) holding time



increased with temperature increasing. At temperatures greater than 900°C, the volatilization rate of zinc clearly increased. When the temperature exceeded boiling point of zinc, 907°C, the volatilization rate of zinc increased sharply, as expressed in Fig 5(b). Furthermore, after the temperature was 910°C, the partial pressure of carbon monoxide was maximum (Fig 5(b)), enhancing Eq. 3. In result, the reduction of zinc oxide was promoted, producing lots of zinc vapor, thus the volatilization rate of zinc increased sharply. This is step with the aforementioned thermomechanical analysis.

Fig 8 shows the effect of the temperature on the removal rate of sulfur. The removal rate of sulfur increased with the increase of temperature. Little sulfur was removed at temperatures lower than 1100°C. The removal rate of sulfur increased rapidly at temperatures higher than 1100°C. The maximum

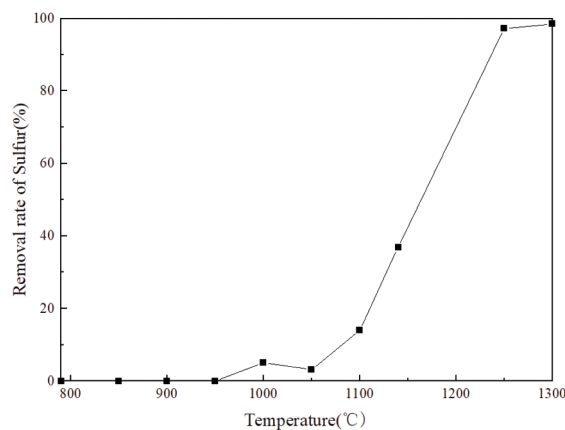


Figure 8. Effects of temperature on removal rate of sulfur

removal rate of sulfur exceeded 97% at 1300°C. This is analogous to the variation tendency of zinc, as expressed in Fig 7(a); hence, sulfur might be related to the behavior of zinc to some extent. Fig 9 was the XRD patterns of residues from the temperature experiments. Most zinc oxide was reduced at 1000°C through Eqs. 1 and 3; meanwhile, the X-ray diffraction peak of zinc sulfide was enhanced obviously, meaning that zinc sulfide was generated in the residue through Eqs. 5 and 6. This indicated that sulfur could hinder the reduction of zinc oxide by capturing zinc, and decrease volatilization rate of zinc because of the higher boiling point of zinc sulfide than metallic zinc. At 1300°C, there was no zinc sulfide in the residue, which demonstrated that zinc sulfide volatilized or was consumed through Eq. 7. Researchers reported that zinc sulfide begins to volatilize at approximately 1178°C [36].

3.2.2. Effect of reductant dosage on zinc volatilization

The effect of reductant dosage on volatilization

rate of zinc was investigated at a holding time of 120 min and a temperature of 1100°C. The reductant dosage was set at 11.48%, 12.76%, 14.04%, 15.95%, 17.23%, and 19.14%. Fig 7(b) shows the effect of reductant dosage on the volatilization rate of zinc.

As the reductant dosage increased, the volatilization rate of zinc decreased and the mass fraction of zinc in the residue increased. The main reason was that the reductant dosage was surplus, more reductant unreacted existed in the residue with increasing reductant dosage. 12.76 wt.% reductant dosage is suitable for the ZOD in laboratory scale. However, the excess coefficient of reductant is 0.1 in most zinc smelting plants; thus, 14.04 wt.% reductant dosage is a more practical condition.

3.2.3. Effect of holding time on zinc volatilization

The effect of holding time on volatilization rate of zinc was investigated at a temperature of 1100°C and reductant dosage of 14.04%, and the holding time was set at 30 min, 60 min, 90 min, 120 min, and 180 min. The result is given in Fig 7(c).

Fig 7(c) shows the volatilization rate of zinc increased from 83.12% to 88.33% and the mass fraction of zinc in the residue decreased from 14.84% to 12.75% when the holding time increased from 30 min to 60 min. However, when the holding time increased to 90 min, the volatilization rate of zinc decreased to 85.69% and the mass fraction of zinc in residue increased to 13.33%. The main reason was that the pressure difference between the reactor and the three-level condensers decreased gradually and some zinc vapor returned to the reactor. After 90 min, the volatilization rate of zinc and mass fraction of zinc in the residue increased and decreased respectively over time. This was because Eq. 3 was gradually complete. In addition, most zinc in the ZOD had volatilized before 30 min, which demonstrated Eqs. 1 and 3 were almost complete within 30 min. In industry, the condensation of zinc vapor is fast, resulting in almost constant pressure difference between the reaction area and the condensation area. Hence, there is no return of zinc in industry. To increase the volatilization rate of zinc as much as possible, 120 min is the optimal condition considering the actual industrial manufacture.

In summary, the optimal reduction conditions were temperature of 1300°C, the reductant dosage of 14.04%, and the holding time of 120 min.

3.2.4. Composition of the slag in the reactor residue at 1300°C

The residue from the experiment (3.3.1) at 1300°C was separated into lead-tin alloy and slag.

Fig. 9 shows the SEM-EDS analysis of slag at



1300°C. The spots 1 and 2 were Al–Si–Ca compounds, and spots 3 and 4 were reductants. There was no zinc sulfide in the slag, which indicated zinc sulfide was consumed through Eq. 7 or volatilized, and the main components of the slag were Al–Si–Ca compounds and the rest reductant. The volatilization rate of zinc was approximately 99% at 1300°C; thus, the formation of zinc sulfide did not affect zinc volatilization. Additionally, the disappearance of zinc sulfide decreases sulfur content of slag, which is beneficial to controlling the slag type.

3.3. “Pelletizing - Calcination-Carbothermic reduction” experiment

The “Pelletizing - Calcination-Carbothermic reduction” experiment was conducted under the optimal reduction condition.

3.3.1. Calcination process

As shown in Fig. 1 and Table 1, some fluorine, chlorine, and sulfur elements existed in the dust, and

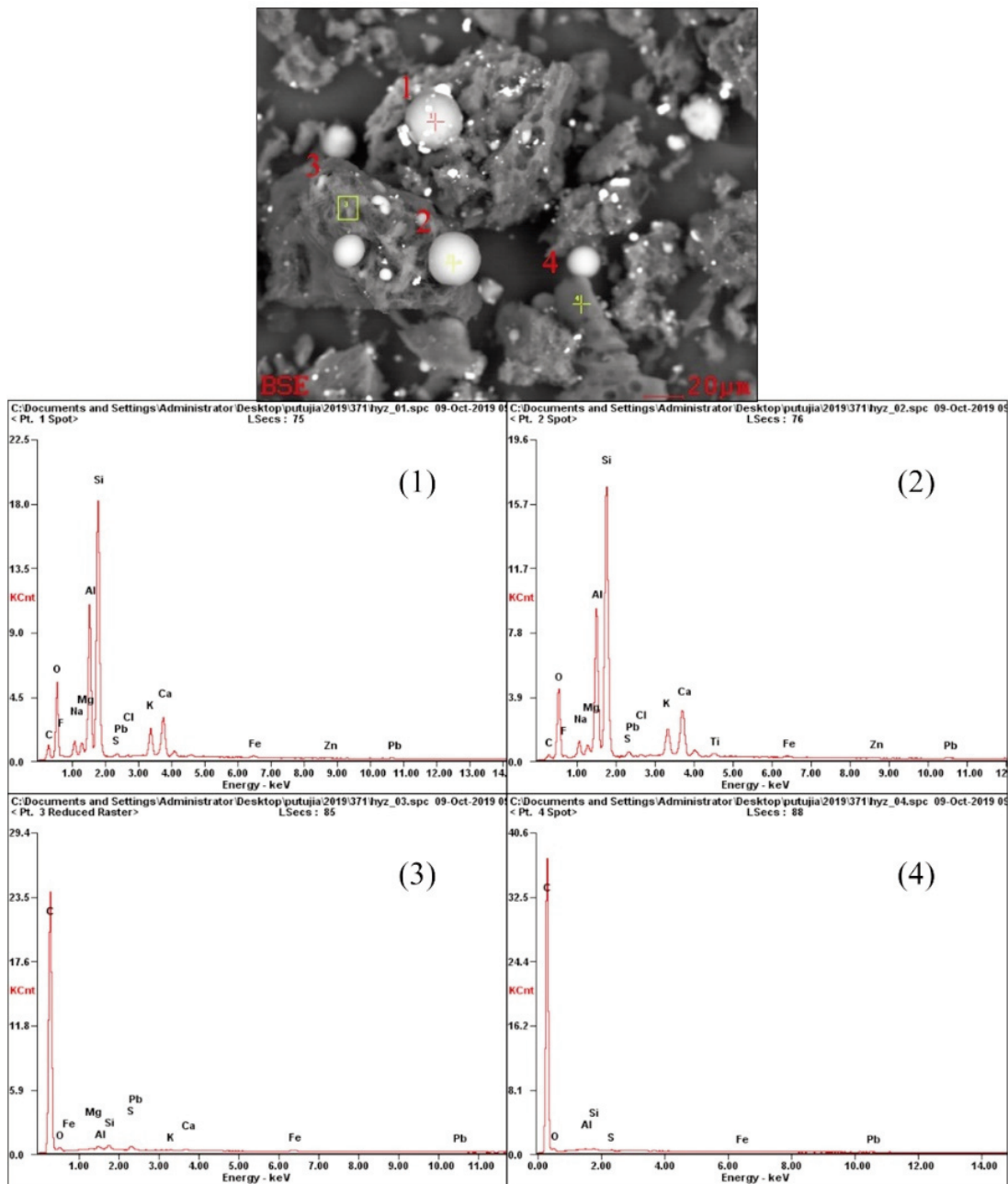


Figure 9. SEM-EDS results of the slag at 1300°C



some fluorine and chlorine combined with lead to form $PbFCl$, which would cause the decrease of direct recovery of valuable elements during the carbothermic reduction process. Therefore, the purpose of the calcination process was to remove fluorine, chlorine, and sulfur before the carbothermic reduction process. The results were shown in Table 3.

Table 3. Results of calcination process (wt.%)

| Removal rate of impurities | | | Volatilization rate of valuable elements | | |
|----------------------------|-------|-------|--|------|-------|
| F | Cl | S | Zn | Pb | Sn |
| 98.18 | 96.38 | 28.58 | 0.87 | 4.17 | <0.01 |

Table 3 indicated that most fluorine and chlorine were removed, and the removal rate of sulfur was 28.58% after calcination. Meanwhile, the volatilization rate of valuable elements was low, which was beneficial for the recovery of valuable elements.

3.3.2. Carbothermic reduction process

The results found that the residue in the reactor and the condensate in the three-level condensers were 174.6 g and 383.8 g, respectively, and the volatilization rate of zinc was 99.83%. After the separation of the residue and condensate, 23.0 g slag, 149.8 g lead-tin alloy, 340.8 g crude zinc, and 43.0 g condensation powder were obtained. The X-ray diffraction analysis of the three solid products is shown in Fig. 10. As shown in Fig. 10(c), the condensation powder was a mixture of zinc oxide, zinc sulfide, and zinc. During the carbothermic reduction process, zinc vapor and some zinc sulfide entered into three-level condensers, and some zinc vapor was oxidized by air or carbon dioxide to form zinc oxide [37].

In EAF method, the lead splash condenser is used for the condensation of zinc vapor, and the condensation efficiency is more than 94%. It can achieve primary separation of metallic zinc and lead, and can effectively avoid the secondary oxidation of zinc vapor. The liquid zinc from the lead splash condenser can be sent to the refining system to make refined zinc. The slag could be sold as cement raw material.

3.3.3. Mass balance of zinc

The mass balance of zinc in the solid products after carbothermic reduction process was shown in Table 4.

As shown in Table 4, the distribution rate of zinc in the slag was 0.08%, meaning that zinc in the dust was extracted efficiently. The distribution rate of zinc in

the crude zinc was 57.71%, and the zinc content of crude zinc was 68.48%. Section of the crude zinc was gray with an obvious metallic luster. Crude zinc was essentially a kind of lead-zinc alloy (Fig 10(a)). Metallic lead was entrained by zinc vapor and melted into crude zinc in three-level condensers, which was the reason for the generation of crude zinc. In addition, the distribution rate of zinc in the condensation powder was 4.69%. Some zinc vapor was deoxidized by carbon dioxide or air and

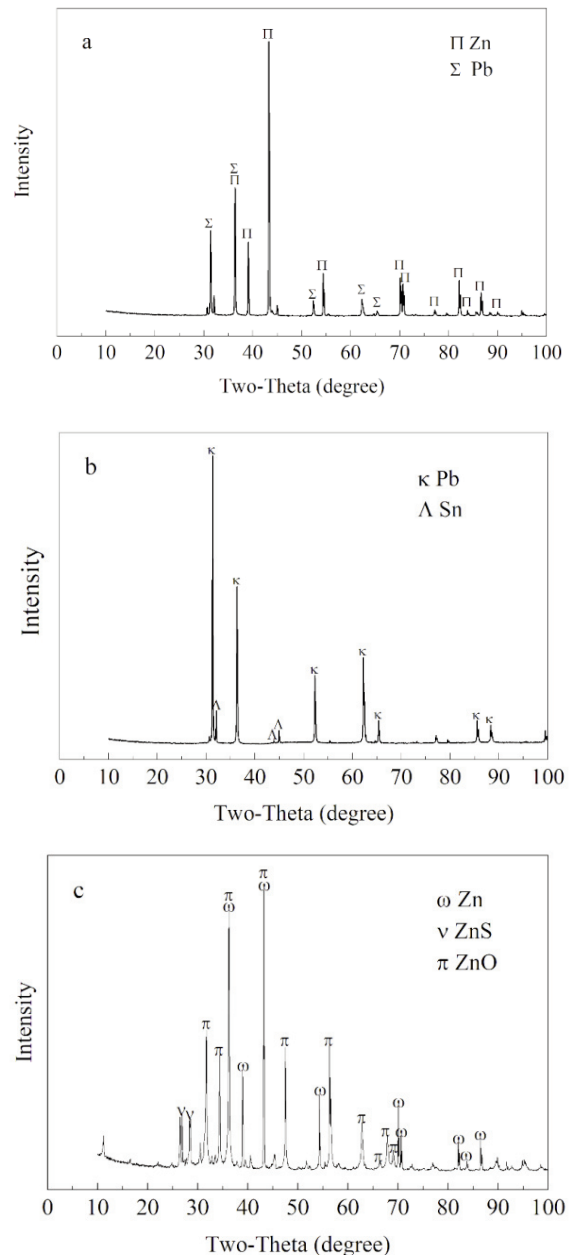


Figure 10. X-ray diffraction analysis of the (a) crude zinc, (b) lead-tin alloy, (c) condensation powder

Table 4. Mass balance of zinc

| Destination | Total mass/g | Composition | Mass/g | Zinc content/% | Mass of zinc/g | Distribution rate/% | Actual picture |
|---------------------------|--------------|-----------------------------------|----------------|----------------|-----------------|---------------------|---|
| Residue in reactors | 174.00 | Slag Lead-tin alloy | 23.00 149.8 | 1.49 0.23 | 0.34 0.34 | 0.08 0.09 |   |
| Condensates in condensers | 383.30 | Condensation powder Crude zinc | 43.00 340.8 | 44.07 68.48 | 18.95 233.37 | 4.69 57.71 |   |
| Loss | / | Loss | / | / | 151.38 | 37.43 | / |

converted into zinc oxide powder before condensation [37]. Zinc sulfide produced by Eq. 5 and 6 volatilized and formed a powder in the three-level condensers.

3.3.4. Effect of sulfur on zinc collection behavior

Table 5 shows the mass balance of sulfur, which indicates that 83.38% of the sulfur in the ZOD volatilized, and 12.21% was collected in the form of zinc sulfide. This indicated that sulfur hindered the reduction of zinc oxide, and the other reason for the loss of zinc might be the volatilization of zinc sulfide.

Table 5. Mass balance of sulfur

| Destination | Total mass/g | Composition | Mass/g | Sulfur content/% | Mass of sulfur/g | Distribution rate/% |
|---------------------------|--------------|-----------------------------------|-----------------|------------------|------------------|---------------------|
| Residue in reactors | 174.00 | Slag Lead-tin alloy | 23.00 149.80 | 2.44 0.58 | 0.56 0.87 | 1.72 2.67 |
| Condensates in condensers | 340.80 | Condensation powder Crude zinc | 43.00 340.80 | 9.26 0.00 | 3.98 0.01 | 12.21 0.01 |
| Loss | / | Loss | / | / | 27.17 | 83.39 |

Hence, the existence of sulfur in the dust is adverse to the reduction and recovery of zinc during carbothermal reduction.

4. Conclusions

(1) The zinc in the ZOD could be extracted and recovered efficiently by carbothermic reduction method. Finally, the crude zinc and lead-tin alloy were obtained. This provided certain experimental reference data for the treatment of zinc oxide dust



with high lead content by EAF method.

(2) Temperature was the key factor for zinc volatilization, and the volatilization rate of zinc sharply rose in accordance with increasing temperature. Compared to temperature, the effects of reductant dosage and holding time on the volatilization rate of zinc were weaker. The optimal reduction condition is the temperature of 1300°C, reaction time of 120 min and reductant dosage of 14.04%.

(3) After the calcination at 900°C for 60 min, the removal rates of fluorine, chlorine, and sulfur were 98.18%, 96.38%, and 28.58%, respectively. After the carbothermic reduction, the zinc distribution rates in slag and crude zinc were 0.08% and 57.71%, respectively. The zinc content in the crude zinc was 68.48%.

Acknowledgments

The work was financially supported by National Natural Science Foundation of China (Grant No. 202101AT070091).

Author contributions

F.-G. Lei was the principal investigator. Pro. C. Wei, Pro. G. Fan and Dr. M.-T. Li contributed to the thermodynamic analysis. Dr. M.-T. Li, Dr. Z.-G. Deng and X.-B. Li offered some constructive suggestions about the formulation of experimental scheme. Thanks to all authors for their contributions to this work.

Data availability

The data of this work could be obtained by contacting with the corresponding author by e-mail.

Declaration of competing interest

No potential conflict of interest was reported by the authors.

References

- [1] Y. Luo, L. Zhang, J. Peng, Y. Wang, C. Sun, H. Xia, G. Chen, S. Ju, Status and future trend of fluorine removal in hydrometallurgical process of zinc oxide dust, *China Nonferrous Metallurgy*, 42 (4) (2013) 39-43. <https://doi.org/10.3969/j.issn.1672-6103.2013.04.011> (in Chinese)
- [2] Y. Li, Z. Liu, Q. Li, Z. Zhao, Z. Liu, L. Zeng, L. Li, Removal of arsenic from arsenate complex contained in secondary zinc oxide, *Hydrometallurgy*, 109 (3-4) (2011) 237-244. <https://doi.org/10.1016/j.hydromet.2011.07.007>
- [3] J. Gao, Z. Huang, Z. Wang, Z. Guo, Recovery of crown zinc and metallic copper from copper smelter dust by evaporation, condensation and super-gravity separation, *Separation and Purification Technology*, 231 (2020) 1-8. <https://doi.org/10.1016/j.seppur.2019.115925>
- [4] A. Ma, X. Zheng, J. Peng, L. Zhang, S. Chandrasekar, J. Li, C. Wei, Dechlorination of zinc oxide dust derived from zinc leaching residue by microwave roasting in a rotary kiln, *Brazilian Journal of Chemical Engineering*, 34 (1) (2017) 193-202. <https://doi.org/10.1590/0104-6632.20160331s00003530>
- [5] M. Silwamba, M. Ito, N. Hiroyoshi, C.B. Tabelin, R. Hashizume, T. Fukushima, I. Park, S. Jeon, T. Igarashi, T. Sato, M. Chirwa, K. Banda, I. Nyambe, H. Nakata, S. Nakayama, M. Ishizuka, Recovery of lead and zinc from zinc plant leach residues by concurrent dissolution-cementation using zero-valent aluminum in chloride medium, *Metals*, 10 (4) (2020) 1-15. <https://doi.org/10.3390/met10040531>
- [6] M.K. Jha, V. Kumar, R.J. Singh, Review of hydrometallurgical recovery of zinc from industrial wastes, *Resources Conservation and Recycling*, 33 (1) (2001) 1-22. [https://doi.org/10.1016/S0921-3449\(0\)00095-1](https://doi.org/10.1016/S0921-3449(0)00095-1)
- [7] R.J.E. Martins, V.J.P. Vilar, R.A.R. Boaventura, Kinetic modelling of cadmium and lead removal by aquatic mosses, *Brazilian Journal of Chemical Engineering*, 31 (1) (2014) 229-242. <https://doi.org/10.1590/S0104-66322014000100021>
- [8] A.D. Souza, P.S. Pina, V.A. Leao, Bioleaching and chemical leaching as an integrated process in the zinc industry, *Minerals Engineering*, 20 (6) (2007) 591-599. <https://doi.org/10.1016/j.mineng.2006.12.014>
- [9] Y. Zhao, Q. Li, C. Zhang, J. Jiang, Production of ultrafine zinc powder from wastes containing zinc by electrowinning in alkaline solution, *Brazilian Journal of Chemical Engineering*, 30 (4) (2013) 857-864. <https://doi.org/10.1590/S0104-66322013000400017>
- [10] Z. Peng, G. Dean, C. Wenzl, J.F. White, Slag metallurgy and metallurgical waste recycling, *Jom*, 68 (9) (2016) 2313-2315. <https://doi.org/10.1007/s11837-016-2047-2>
- [11] C. Wang, Y. Guo, L. Yang, F. Chen, Situation and research development of recovery valuable metals in zinc dust and residue, *Metal Mine*, (3) (2019) 21-29. <https://doi.org/10.19614/j.cnki.jsks.201903003> (in Chinese)
- [12] F. Zhang, C. Wei, Z. Deng, C. Li, X. Li, M. Li, Reductive leaching of zinc and indium from industrial zinc ferrite particulates in sulphuric acid media, *Transactions of Nonferrous Metals Society of China*, 26 (9) (2016) 2495-2501. [https://doi.org/10.1016/S1003-6326\(16\)64342-X](https://doi.org/10.1016/S1003-6326(16)64342-X)
- [13] M. Roshanfar, M. Khanlarian, F. Rashchi, B. Motesharezadeh, Phyto-extraction of zinc, lead, nickel, and cadmium from a zinc leach residue, *Journal of Cleaner Production*, (148) (2020). <https://doi.org/10.1016/j.jclepro.2020.121539>
- [14] B. Aparajith, D.B. Mohanty, M.L. Gupta, Recovery of enriched lead-silver residue from silver-rich concentrate of hydrometallurgical zinc smelter, *Hydrometallurgy*, 1-2 (105) (2010) 127-133. <https://doi.org/10.1016/j.hydromet.2010.08.010>
- [15] N.R. Rodriguez, B. Onghena, K. Binnemans, Recovery



- of lead and silver from zinc leaching residue using methanesulfonic acid, *ACS Sustainable Chemistry & Engineering*, 07 (24) (2019) 19807-19815.
<https://doi.org/10.1021/acssuschemeng.9b05116>
- [16] M.D. Turana, H.S. Altundogan, F. Tumen, Recovery of zinc and lead from zinc plant residue, *Hydrometallurgy*, 75 (1-4) (2004) 169-176.
<https://doi.org/10.1016/j.hydromet.2004.07.008>
- [17] G. He, H. Wu, C. Wang, J. Li, Y. Mao, L. Fu, Study on applicability of zinc oxide dust in the process of hydrometallurgy of zinc, *Shanxi Metallurgy*, (6) (2017) 6-10.
<https://doi.org/10.16525/j.cnki.cn14-1167/tf.2017.06.03> (in Chinese)
- [18] L. Gao, Z. Dai, K. Zhang, Q. Liu, Decreasing lead content in wet zinc smelting slag, *Chemical Industry and Engineering Progress*, 36 (12) (2017) 4672-4678.
<https://doi.org/10.16085/j.issn.1000-6613.2017-0595> (in Chinese)
- [19] E. Rudnik, G. Wloch, L. Szatan, Comparative studies on acid leaching of zinc waste materials, *Metallurgical Research & Technology*, 115 (1) (2018) 110.
<https://doi.org/10.1051/metal/2017076>
- [20] K. Xie, H. Wang, S. Wang, Direct leaching of molybdenum and lead from lean wulfenite raw ore, *Transactions of Nonferrous Metals Society of China*, 29 (12) (2019) 2638-2645.
[https://doi.org/10.1016/S1003-6326\(19\)65170-8](https://doi.org/10.1016/S1003-6326(19)65170-8)
- [21] S.J. Hsieh, C.C. Chen, W.C. Say, Process for recovery of indium from ITO scraps and metallurgical microstructures, *materials science and engineering: B*, 158 (1-3) (2009) 82-87.
<https://doi.org/10.1016/j.mseb.2009.01.019>
- [22] H. Sun, W. Sen, Z. Huang, Y. Jiang, C. Yang, C. Sun, Process study of direct leaching of Pb-Zn bearing dust with sulfuric acid, *Nonferrous Metals (Extractive Metallurgy)*, (1) (2014) 5-7,11.
<https://doi.org/10.3969/j.issn.1007-7545.2014.01.002> (in Chinese)
- [23] M. Şahin, M. Erdem, Cleaning of high lead-bearing zinc leaching residue by recovery of lead with alkaline leaching, *Hydrometallurgy*, 153 (2015) 170-178.
<https://doi.org/10.1016/j.hydromet.2015.03.003>
- [24] G. Jiang, B. Peng, Y. Liang, L. Chai, Q. Wang, Q. Li, M. Hu, Recovery of valuable metals from zinc leaching residue by sulfate roasting and water leaching, *Transactions of Nonferrous Metals Society of China*, 27 (5) (2017) 1180-1187.
[https://doi.org/10.1016/S1003-6326\(17\)60138-9](https://doi.org/10.1016/S1003-6326(17)60138-9)
- [25] M. Ye, P. Yan, S. Sun, D. Han, X. Xiao, L. Zheng, S. Huang, Y. Chen, S. Zhuang, Bioleaching combined brine leaching of heavy metals from lead-zinc mine tailings: Transformations during the leaching process, *Chemosphere*, 168 (2017) 1115-1125.
<https://doi.org/10.1016/j.chemosphere.2016.10.095>
- [26] L. Tang, C. Tang, J. Xiao, P. Zeng, M. Tang, A cleaner process for valuable metals recovery from hydrometallurgical zinc residue, *Journal of Cleaner Production*, 201 (2018) 764-773.
<https://doi.org/10.1016/j.jclepro.2018.08.096>
- [27] S. Coruh, O.N. Ergun, Use of fly ash, phosphogypsum and red mud as a liner material for the disposal of hazardous zinc leach residue waste, *Journal of Hazardous Materials*, 173 (1-3) (2010) 468-473.
<https://doi.org/10.1016/j.jhazmat.2009.08.108>
- [28] A. Özverdi, M. Erdem, Environmental risk assessment and stabilization/solidification of zinc extraction residue: I. environmental risk assessment, *Hydrometallurgy*, 100 (3-4) (2010) 103-109.
<https://doi.org/10.1016/j.hydromet.2009.10.011>
- [29] C. Stefanie, G. Alexander, M. Robert, et al., Ausmelt technology for treating zinc residues, *World of Metallurgy - ERZMETALL*, 66 (4) (2013) 230-235.
www.researchgate.net/publication/270048746_Ausmelt_Technology_for_Treating_Zinc_Residues
- [30] A. Ma, X. Zheng, S. Wang, J. Peng, L. Zhang, Z. Li, Study on dechlorination kinetics from zinc oxide dust by clean metallurgy technology, *Green Processing and Synthesis*, 05 (1) (2016) 49-58.
<https://doi.org/10.1515/gps-2015-0041>
- [31] A. Moezzi, A.M. McDonagh, M.B. Cortie, Zinc oxide particles: Synthesis, properties and applications, *Chemical Engineering Journal*, 185 (2012) 1-22.
<https://doi.org/10.1016/j.cej.2012.01.076>
- [32] A. Rückert, M. Warzecha, R. Koitzsch, M. Pawlik, H. Pfeifer, Particle distribution and separation in continuous casting tundish, *Steel Research International*, 80 (8) (2009) 568-574.
<https://doi.org/10.2374/SRI09SP043>
- [33] X. Guo, B. Zhang, H. Yang, A Kinetic of the reduction of ZnO pellets containing graphite, *Journal of Chongqing University*, 25 (5) (2002) 86-88.
<https://doi.org/10.3969/j.issn.1000-582X.2002.05.022> (in Chinese)
- [34] W. Lv, M. Gan, X. Fan, Z. Ji, X. Chen, J. Yao, T. Jiang, Recycling utilization of zinc-bearing metallurgical dust by reductive sintering: Reaction behavior of zinc oxide, *Jom*, 71 (9) (2019) 3173-3180.
<https://doi.org/10.1007/s11837-019-03645-y>
- [35] S. Zhou, Y. Wei, B. Li, H. Wang, Cleaner recycling of iron from waste copper slag by using walnut shell char as green reductant, *Journal of Cleaner Production*, 217 (2019) 423-431.
<https://doi.org/10.1016/j.jclepro.2019.01.184>
- [36] Z. Wang, *Electric furnace zinc smelting*. Metallurgical Industry Press, Beijing, 2006, p. 436. (in Chinese)
- [37] Y. Liu, Y. Du, Q. Li, H. Zhao, Y. Xiao, To study the mechanism of zinc preparation by zinc oxide in vacuum and condensation, *Vacuum*, 53 (3) (2016) 74-77.
<https://doi.org/10.13385/j.cnki.vacuum.2016.03.17> (in Chinese).



DOBIJANJE CINKA KARBOTERMIJSKOM REDUKCIJOM IZ PRAŠINE CINK OKSIDA SA SADRŽAJEM VIŠE METALNIH ELEMENATA

F.-G. Lei ^{a,b,c}, M.-T. Li ^{a,*}, C. Wei ^a, Z.-G. Deng ^a, X.-B. Li ^a, G. Fan ^a

^a Fakultet za metalurško i energetsko inženjerstvo, Univerzitet nauke i tehnologije u Kunmingu, Kunming, Kina

^b Glavna državna laboratorija za sveobuhvatnu primenu refraktornih ruda sa niskim sadržajem zlata, Ksiamen, Kina

^c Zidiin Majning Ksiamen Zidiin rudarska i metalurška tehnologija Co,Ltd., Ksiamen, Kina

Apstrakt

Proces karbotermijske redukcije koji simulira EAF proces korišćen je za obradu prašine cink oksida iz koje cink može biti efikasno dobijen. Sirovi cink i legura olova i kalaja su dobijene na kraju. Ispitivani su uticaj temperature, vremena trajanja i doziranje reducenata na brzinu isparavanja cinka, i urađen je eksperiment "Peletiranje – kalcinacija – karbotermička redukcija". Rezultati su otkrili da je optimalni redukcionni uslov sledeći: temperatura 1300 °C, doza reducenta 14.04%, i vreme trajanja 120 min. Posle kalcinacije na 900°C u trajanju od 120 min, stopa uklanjanja fluora, hlora i sumpora iz prašine bila je 98.18%, 96.38% i 28.58%, pojedinačno, a stopa isparavanja cinka u procesu redukcije je bila 99.83%. Sadržaj cinka u sirovom cinku bio je 68.48%.

Ključne reči: Prašina cink oksida; Karbotermijska redukcija; Isparavanje; Kondenzacija; Iskorišćenje

